CHAPTER TWO

Physics of the Fall

In the following, we shall examine the phenomena associated with the collision between Earth and a small celestial body. While data for the penetrating body must be acquired by observation during the actual fall, the pertinent data for Earth are already available. The Earth revolves about the Sun in an almost circular orbit; see Table 1. Its direction is direct, and its average heliocentric velocity is

$$v_E = \sqrt{\frac{GM}{a}} = \sqrt{\frac{(6.67 \cdot 10^{-8}) \cdot (1.99 \cdot 10^{33})}{149.6 \cdot 10^{11}}}$$

$$= 29.8 \text{ km/sec}$$

G is the universal (Gaussian) gravitational constant in $\text{dyn} \cdot \text{cm}^2 \cdot \text{g}^{-2}$, M is the mass of the Sun in grams, and a is the semimajor axis of the Earth orbit, in centimeters.

Just as an object must have the escape velocity if it is to overcome Earth's gravity, so it will gain this same velocity when it enters the region where Earth's gravitational field is dominant. A body originating from outside Earth's environment will, therefore, acquire an additional velocity equal to the escape velocity when it approaches Earth. At a height of 50-100 km, for example, where meteor velocities are determined, the escape velocity is 11.2 km/sec, and this is the gravitational component which must be subtracted from the measured velocity, v_∞, in order to obtain the geocentric velocity, v_G, of the object:

$$v_G^2 = v_\infty^2 - 11.2^2 = v_\infty^2 - 125$$

As an interesting result of this relation, we notice that even if the meteor had no original motion with respect to the Earth ($v_G = 0$), the Earth's attraction would make it strike the atmosphere at 11.2 km/sec. The effect of the rotation of the Earth will also have to be taken into account for accurate studies of meteor velocities. Since Earth's rotational velocity at Equator is (only) 0.47 km/sec, the maximum correction is small compared to other values.

When v_G has been determined, it must be combined with v_E to give v_H, the heliocentric velocity of the impacting body, i.e. its orbital velocity with respect to the Sun at the time of impact, Figure 9. At the time of impact, radius vector of the meteoroid orbit equals the Sun-Earth distance, and consequently

$$v_H = \sqrt{GM\left[\frac{2}{1} - \frac{1}{a}\right]} = 29.8 \sqrt{2 - \frac{1}{a}} \text{ km/sec} ,$$

from which equation the semimajor axis of the meteoroid orbit can be calculated.

The equation indicates that, at the time of impact, meteoroids with orbits similar to Earth's ($a = 1$) will display heliocentric velocities about 30 km/sec, while meteoroids in parabolic orbits, for which $a \to \infty$, will have

$$v_H = 29.8\sqrt{2} = 42.1 \text{ km/sec}$$

While it was formerly believed that a great many meteoroids had heliocentric velocities of 42 km/sec and above (Niessl 1925; Hoffmeister 1937; Nielsen 1943), it is now firmly established that almost all bodies penetrating our atmosphere have been moving in elliptical orbits ($29.8 < v_H < 42.1$ km/sec) around the Sun and thus were permanent members of our solar system. A catalog of 1345 bright meteors, some of them meteorite-casting, has been published by Nielsen (1968). Apart from a very few cases, all trajectories have been calculated on the basis of visual observations of fireballs between 1850 and 1965. The development of the photographic technique and the radar technique has now opened new possibilities, and it appears that the catalog will be definitive, its contents displaying the amount of knowledge of bright meteors accumulated at the moment when a new era of meteor study is beginning.

Observational Data on Meteors, Fireballs and Meteorites

One of the most important observed parameters of a meteor is evidently its velocity v_0 in the atmosphere. Unfortunately, the velocity is very difficult to estimate by visual methods, due to various geometric and psychological factors. Several experiments with inexperienced observers have, for example, indicated that the observers extended the meteor's path backwards, thereby exaggerating the height at which it appeared. Extreme values, above 130 km, are very rare on photographs and are now generally regarded with suspicion. Another difficulty liès in the fact that a meteor is best seen near the end of the visible trajectory, where it has already been significantly decelerated by the Earth's atmosphere. In order to distinguish between elliptical, parabolic and hyperbolic orbits, we must, however, have reliable data for the velocities. In recent years astronomers have, therefore, resorted to systematical photography, establishing multiple station

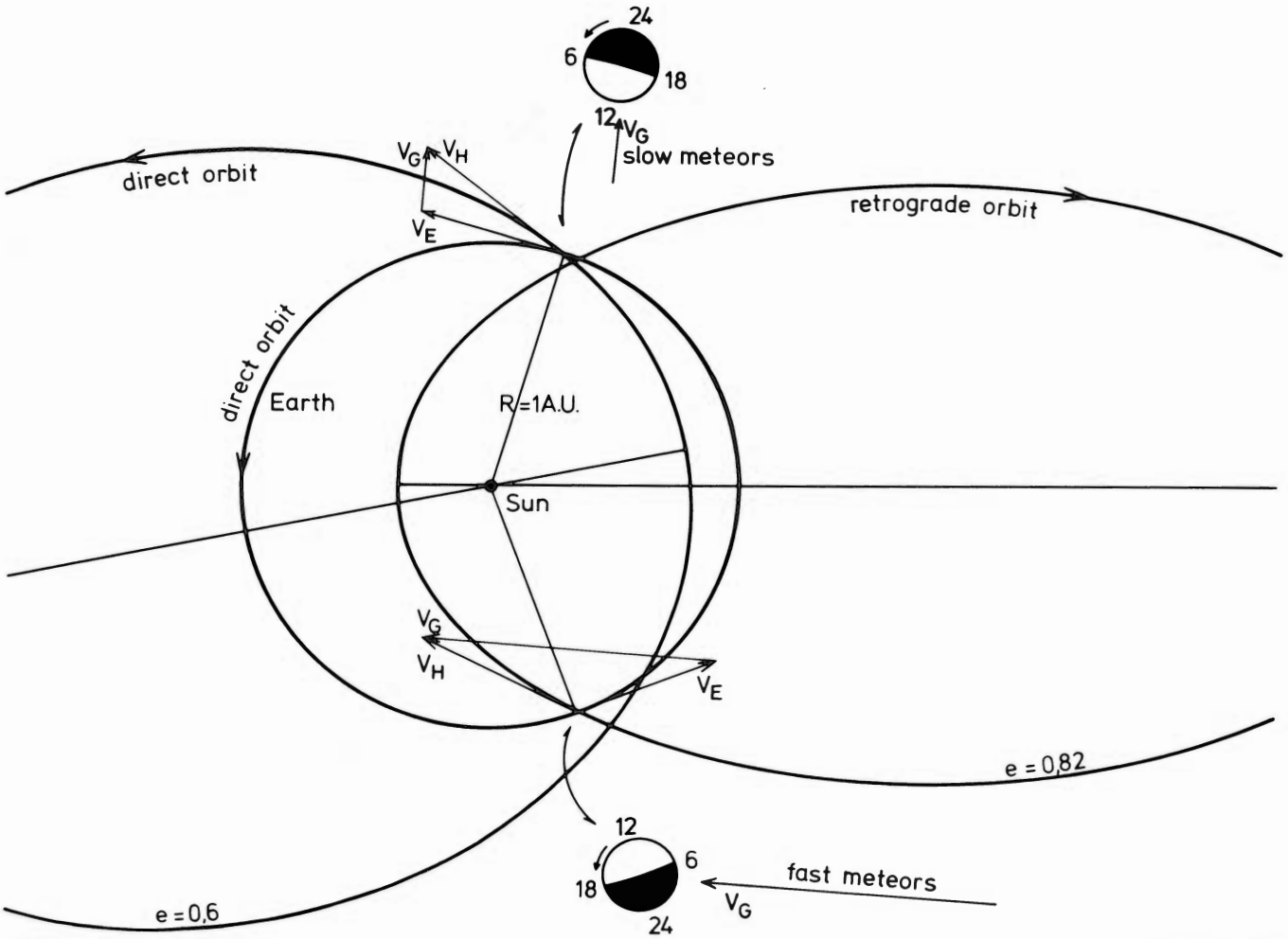

Figure 9. Two hypothetical meteors, one in a direct and one in a retrograde orbit. The geocentric velocity – i.e., the velocity relative to Earth at the time of collision – is obtained by vectorial addition of the heliocentric velocities of Earth (v_E) and the meteorite (v_H). From the sketch it is obvious that fast meteors will occur mainly in the morning hours.

scanning of selected parts of the sky. In Table 5 typical data are compiled from accurately calculated orbits, as determined by photographs from various stations in the USSR.

In 1959, a fireball of magnitude -19 passed in front of 11 meteor cameras in Czechoslovakia, then fell at the town of Přibram, near Prague. From the negatives it was possible to deduce the accurate trajectory and velocity in the atmosphere and, from these data, to calculate with great accuracy the preterrestrial orbit of the body. Nineteen fragments, totaling 9.5 kg were recovered, and the material was shown to be a normal olivine-bronzite chondrite (Tuček 1961; Ceplecha 1961; Hey 1966: 391).

Table 5. Orbital Elements of Selected Meteors Photographed in Tadjikistan, about 40°N, 70°E (Babadjanov 1963)

No.	Day	Month	U.T.	True Radiant			km/sec			Orbital Elements					Note
				α	δ	ϵ	V_∞	V_G	V_H	a	e	q	Q	i	
580065	16	1	1405	52.6	64.7	121.6	18.8	15.2	40.4	5.11	0.814	0.948	9.27	15.4	
580212	10	2	1716	173.8	8.8	60.1	41.1	39.8	35.6	1.68	0.960	0.067	3.29	20.6	
581663	25	6	2221	9.3	18.2	17.8	62.2	61.0	34.2	1.54	0.484	0.797	2.28	155	
570707	26	7	1848	294.8	-7.1	98.0	45.7	44.3	56.5	-0.62	1.89	0.547	-1.78	17.1	hyperbolic
570804[C]	27	7	2006	304.2	-7.5	90.0	24.6	22.0	36.7	2.20	0.734	0.585	3.81	8.9	
582655[P]	13	8	2201	50.5	58.2	40.2	60.4	59.2	41.3	19.9	0.953	0.938	38.9	113	
582995	7	9	1816	286.6	-44.8	145.4	13.2	7.3	35.9	1.87	0.470	0.991	2.75	4.4	
583371	14	9	2142	92.7	26.6	6.0	60.4	59.1	29.8	1.01	0.189	0.821	1.20	173.6	
584412[T]	17	11	1918	62.8	23.3	80.4	29.2	26.9	36.9	2.05	0.809	0.391	3.71	2.2	

C – Capricornid. P – Perseid. T – Taurid. U.T. – universal time, based on the Greenwich meridian and counting from midnight. α – rectascension. δ – declination. ϵ – elongation. V_∞ – meteor velocity before deceleration by the atmosphere. V_G – geocentric velocity. V_H – heliocentric velocity. a – semimajor axis, A.U. e – eccentricity. q – perihelion distance, A.U. Q – aphelion distance, A.U. i – inclination in degrees.

A systematic effort has recently been made by several countries to photograph the fireballs caused by objects large enough to reach the ground intact so that their former orbits and landing points can be calculated. In 1964 the All Sky Network, covering Czechoslovakia and part of Germany, was established. In Western Canada a network of 12 observatories surveys 600,000 km^2 of land, terrain which is readily accessible for the searching of meteorites (Blackwell & Halliday 1969). The Prairie Network in the U.S.A. was put into operation in 1965 and effectively covers about 10^6 km^2 (McCrosky & Ceplecha 1969). It was organized by the Smithsonian Astrophysical Observatory and comprises a system of 16 automated camera stations dispersed over the Plains States, where the recovery of a fallen meteorite is potentially easiest. A report on 100 photographically observed fireballs and their accurately calculated preterrestrial orbits has been published by McCrosky (1968), and from this report a few selected data are given in Table 6. On January 9, 1970, the Lost City meteorite was located as a result of the photographic coverage from two stations in the network (McCrosky 1970; McCrosky et al. 1971; Clarke et al. 1971b). Lost City is the first meteorite with a precisely known orbit which has been immediately studied for its shortlived radioisotopes, caused by cosmic irradiation. See also Figure 1.

Data for Přibram, Lost City, Sikhote-Alin and a few other imposing fireballs believed to have been caused by potential meteorites are compiled in Table 7. Comparison with the data in Tables 5 and 6 indicates that the geocentric and atmospheric velocities are consistently small. Similarly, in spite of a fair range in semimajor axes and eccentricities, the inclinations of the orbits are low and all movements are counterclockwise, like that of the planets. The average velocity, v_∞, for the nine fireballs in Table 7 is 16.9 km/sec. This is in accordance with the study by Whipple & Hughes (1955) who estimated the average velocity of meteorites in the Earth's atmosphere to be 17 km/sec.

To illustrate how meteoritic orbits fit in with orbits of other objects in the solar system, Kresak (1968) has proposed the plotting of semimajor axis/eccentricity diagrams. A slightly modified version, prepared by Millman (1970) is shown as Figure 11. The small dots, clustered mainly at the left of the diagram, represent the asteroids, while the open circles, near the center of the plot, are the comets. The ovals in broken lines correspond to some of the major meteor showers. The two heavy curved lines mark the boundaries of the area of the figure where intersection with the Earth's orbit is at all possible ($a(1 - e) < 1 < a(1 + e)$). The thin curved full line is Whipple's criterion (1954) for separating comets from asteroids and the broken curved line, a revised criterion suggested by Kresak (1968).

The nine large numbered dots in the diagram correspond to the objects listed in Table 7. It will be noted that they fall in the same general range as some of the anomalous asteroids (Table 3). Both the Apollo asteroids and the Mars asteroids outside the asteroid belt proper (a<2.1 A.U.) have short capture life times compared to the

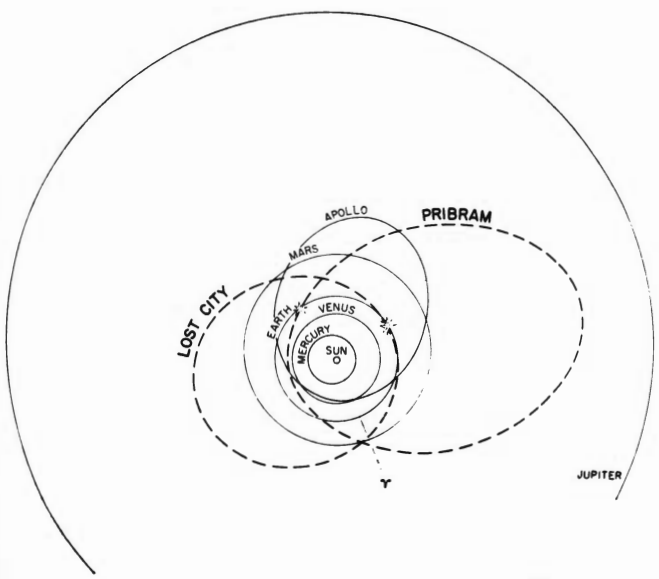

Figure 10. Orbits for the stone meteorites Pribram (H5) and Lost City (H5) as calculated from photographs of the meteorite paths in the atmosphere.

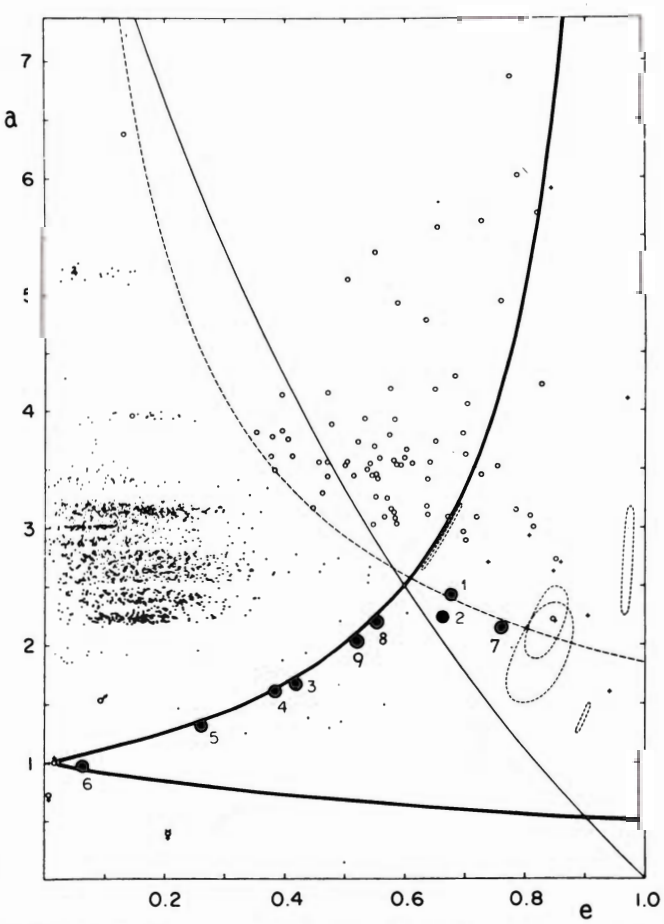

Figure 11. The semimajor axis, a, plotted against eccentricity, e, for various objects in the solar system. ♁ = Earth, ♀ = Venus, ☿ = Mercury, ♂ = Mars, ♃ = Jupiter. The nine numbered dots correspond to the bodies listed in Table 7. (Adapted from Whipple 1954; Kresak 1968; and Millman 1970.)

Table 6. Orbital Elements of Some Fireballs in the Brightness Range −5 to −18 photographed from the Prairie Network, about 40°N, 95°W (McCrosky 1968)

No.	Day	Month	U.T.	True Radiant		km/sec			Orbital Elements				
				R.A.	Declin.	V_∞	V_G	V_H	a	e	q	Q	i
39499	9	1	0753	3.6	21.3	12.6	6.58	36.84	1.99	0.50	0.98	2.99	0.9
38469	15	3	0702	-10.7	178.8	33.0	31.10	39.55	4.08	0.90	0.39	7.76	12.3
39276	31	5	0737	-9.5	247.4	25.8	23.43	38.08	2.97	0.79	0.60	5.34	9.3
39349P	12	8	0326	57.1	45.0	61.0	59.81	41.55	40.20	0.97	0.96	79.4	114.4
39360	23	8	0450	-17.9	16.6	24.0	20.93	24.74	0.77	0.66	0.25	1.29	25.0
39434D	5	11	1042	-3.7	167.2	14.6	9.03	23.47	0.71	0.43	0.40	1.02	3.3
39080L	16	11	0604	22.7	152.5	72.5	71.33	42.14	52.6	0.98	0.98	104	161.8
39086T	22	11	1108	24.3	66.3	28.5	26.55	37.33	2.20	0.81	0.41	3.99	2.7
39470D	11	12	0112	24.1	75.7	23.6	20.46	37.22	2.13	0.71	0.61	3.66	0.8

P – Perseid L – Leonid T – Taurid D – detonating bolide

Table 7. Orbital Elements of Nine Asteroidal Type Meteoroids (Three Meteorites and Six Fireballs)

	Year	Day	Month	Local Time	True Radiant		km/sec			Orbital Elements					No. on Figure 11
					α	δ	V_∞	V_G	V_H	a	e	q	Q	i	
Meteorites															
Sikhote-Alin (iron) USSR[7]	1947	12	2	10:38	28	80	14.5	9.2	37	2.16	0.54	0.99	3.34	9.4	8
Pribram (stone) Czechoslovakia[1]	1959	7	4	20:30	191.5	17.7	20.9	17.5	37.5	2.42	0.67	0.79	4.05	10.4	1
Lost City (stone) Oklahoma[4]	1970	3	1	20:14	315.0	39.1	14.2	8.7	35.1	1.66	0.42	0.96	2.36	12.0	3
Fireballs															
No. 1242, Harvard[2]	1945	6	2	0:12	3.0	59.2	12.2	4.8	33.4	1.33	0.26	0.98	1.68	6.9	5
Fireball, Alberta[6]	1956	1	11	6:00	332	73.2	13.0	6.6	29.8	1.00	0.06	0.94	1.06	12.8	6
No. 19816, New Mexico[2]	1958	8	12	1:50	70.5	-0.2	20.7	17.4	37.0	2.24	0.66	0.76	3.72	12.6	2
No. 27471, Ondrejov[3]	1960	27	10	1:13	39.1	10.9	26.0	23.5	36.5	2.08	0.76	0.50	3.66	4.9	7
Fireball, New York-Quebec[5]	1966	25	4	19:14	137.9	-57.7	17.0	12.8	34.8	1.60	0.38	0.98	2.21	20.0	4
No. 40617, Prairie Network[8]	1970	31	1	3:00	62.1	37.6	13.2	7.1	36.5	2.02	0.52	0.98	3.06	3.3	9

1) Ceplecha 1961.
2) Cook et al. 1963.
3) Ceplecha & Rajchl 1963.
4) McCrosky et al. 1971. The fall of Lost City went unobserved. Had it not been for the automatic cameras, this stone meteorite fall might not have been recognized at all.
5) Griffin 1968.
6) Halliday 1960, as revised by Millman 1970.
7) Fesenkov 1951a,b.
8) McCrosky et al. 1971.

age of the solar system (Öpik 1963). They must be replenished from some source, presumably the Mars asteroids in the region 2.2-2.8 A.U. (Anders 1964). Traversing the main part of the asteroid belt during each revolution, they will suffer impacts from time to time. The debris, being ejected with low velocities, will move in similar Mars-crossing orbits, but of slightly different periods. Consequently it will soon spread out in a toroid along the orbit of the parent body. Secular perturbations will further disperse the debris, and close encounters with Mars will reorient the velocity vectors of the debris, leading to Earth-crossing orbits in a small percentage of cases and thus act as a source of meteorites (Öpik 1951; Arnold 1965; Anders 1971c).

The Přibram meteorite, No. 1 on Figure 11, is situated near the dividing line between cometary and asteroidal objects. Its trajectory and associated light phenomena have been described by meteor astronomers as caused by a

typical low-density (i.e. <1), fragile cometary object, and yet the immediate search yielded 10 kg of a typical stone chondrite (density ~ 3.5). The Přibram paradox, which has been described by, e.g. McCrosky & Ceplecha (1969), is still unsolved. Perhaps such objects exist in space that represent transitional phases between comets and asteroids. "Several astronomers feel that some of the minor planets (i.e. asteroids) may be defunct cometary nuclei. The number of minor planets that are old comets may not be very large (less than 0.1% ?); but if there are indeed any, they should be taken into consideration when we formulate ideas concerning the origin and evolution of the solar system" (Marsden 1970). As possible candidates for comets that turn into asteroids or at least into objects that look like them, Marsden suggested Arend-Rigaux, Neujmin 1 (Table 4) and perhaps some of the Apollo asteroids. Hindley (1971) has also recently discussed the associated problems.

The paradox may, however, also be caused by our imperfect understanding of the supersonic flight in the atmosphere and particularly by our lack of knowledge of the initial shape and size of the impacting meteoroids.

The Meteorite Fall

In outer space meteorites are far too small objects to be observed from telescopes based on Earth. Once they enter the Earth's atmosphere, however, their presence is made manifest by violent light and sound effects. Small meteors, with their low coherence and density, are extinguished at high altitudes and display no sound phenomena, and hardly anything except dust, oxidized microparticles and gases ever reach the ground. Larger meteors produce fireballs, associated with sound and trail phenomena (see, e.g., Nielsen 1968) but again, per definition, nothing reaches the surface of the ground as tangible objects.

The meteoritic masses that survive the fall and are recovered may be extremely small. Revelstoke, for example, a stone meteorite that fell on March 31, 1965, in a remote area of British Columbia, Canada, yielded only two small fragments, totaling one gram, although the fireball was observed to travel for 100 km, and violent detonations were heard up to 130 km away. The fall was even recorded on seismographs 400 km distant (Meteoritical Bulletin, No. 34, 1965).

If we consider iron meteorites alone (see Figure 12), masses of 10-40 kg are most commonly recovered, while upper and lower limits are 60 tons (Cape York, Hoba) and a few hundred grams (Wedderburn, Freda, Föllinge), respectively. Larger masses have occasionally hit the surface of the Earth but have disintegrated during a cratering impact (Canyon Diablo, Wabar, Kaalijärv, etc. Table 18), and only minor surviving samples can now be discovered around the craters. Iron meteorites smaller than 210 g have not been collected as the end product of an individual fall; small masses are nevertheless common as distorted, wedge-shaped

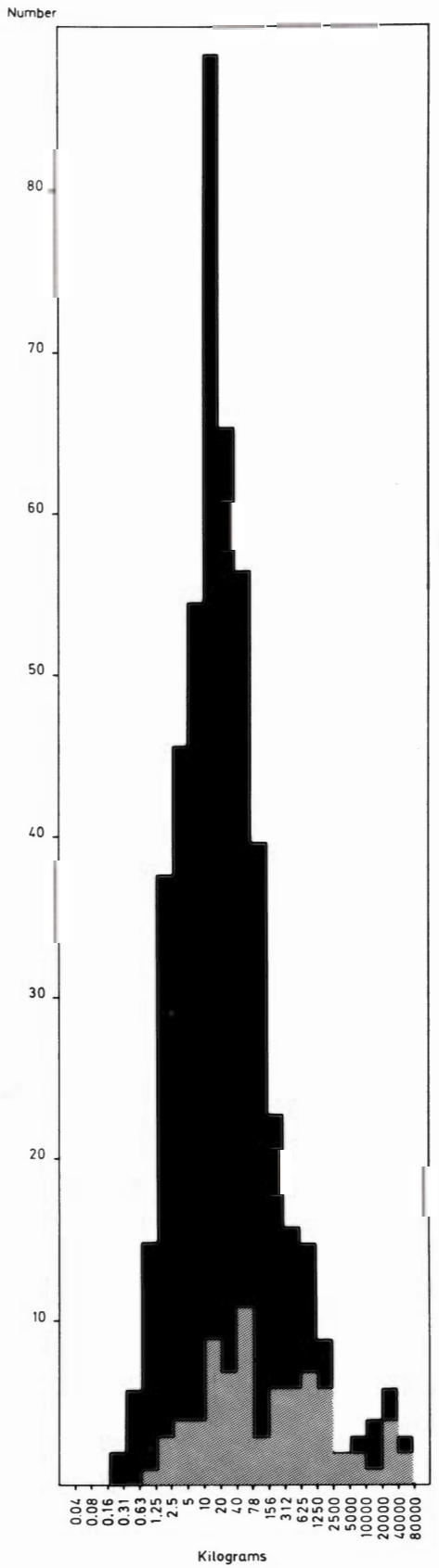

Figure 12. Histogram that shows the number of recovered iron meteorites within each mass range. Black indicates the total number analyzed (495), while gray indicates such events (78) which are known to have caused meteorite showers or craters, such as Toluca and Canyon Diablo.

fragments from cratering impacts, particularly from Canyon Diablo and Henbury.

The flight of meteors and meteorites in our atmosphere has been the subject of numerous treatises, and several physical and mathematical models have been suggested. Calculations which are historically interesting were presented at an early date by Le Conte (1872), Schiaparelli (1908) and Niessl (1925). Elaborate treatments of the physics of the fall – and of reentry of satellites – have been presented by Hoppe (1937), Hoffmeister (1937), Astapovich (1958), Öpik (1958b), Levin (1961), Berman (1961), Duncan (1962), Loh (1963), Blasingame (1964), Martin (1966) and many others. A simplified version will be presented here.

A body approaching Earth from interplanetary space possesses a large amount of energy, potential energy because of its position above Earth's surface and kinetic energy because of its velocity. In most cases the kinetic form predominates. The minimum kinetic energy is, at 11.2 km/sec, 15,000 cal/g. That this energy is not negligible is illustrated by comparison with the energy required to vaporize water, 540 cal/g (at 100° C), and to vaporize carbon, about 13,000 cal/g. The latter is among the highest heats of vaporization of known materials. However, as we have seen, meteors and meteorites may encounter Earth with velocities up to 72 km/sec (Tables 5, 6, 7). In this extreme case the kinetic energy of the impacting body amounts to 620,000 cal/g.

If all of the body's kinetic energy were converted into thermal energy within the body itself, it would thus be more than sufficient to vaporize it entirely. In actual fact, the body's initial energy is transformed, through the mechanism of gas-dynamic drag, into thermal energy in the surrounding air, and only a small fraction of this energy is transferred to the body as heat. This fraction depends upon the flight characteristics.

Newton showed that the drag force, F, is opposite to the direction of movement and proportional to the density of the air, ρ, and the velocity squared, v^2:

$$F = \text{constant} \cdot \rho v^2$$

It is now conventional to use the law in the following forms:

$$F = m \frac{dv}{dt} = - DA \rho v^2$$

or

$$\frac{dv}{dt} = - \frac{DA}{m} \rho v^2 = - \frac{D \pi r^2}{\frac{4}{3} \pi r^3 d} \rho v^2 = - \frac{3}{4} D \frac{\rho v^2}{rd} \quad (1)$$

where m is the mass of the meteorite, A its cross-sectional area, r its radius, d its density and dv/dt its deceleration during flight. D is a drag coefficient, a form factor, which will vary with the exact conditions of the meteorite shape and velocity but usually lies between 0.4 and 1.4.

As the meteorite approaches Earth it first encounters an atmosphere of low density. As it penetrates below 100 km, the density increases rapidly, and as a result of drag, the velocity begins to decrease. Simultaneously, the mass and cross sectional area decrease due to ablation, i.e., radius decreases in equation (1). Thus the deceleration is the product of three quantities, one increasing and the two others decreasing. Initially the deceleration increases, but at some point the velocity begins to decrease more rapidly than the increase in density, resulting in a maximum on the deceleration curve, that for vertical infall will, for example, approach 300 times gravity at 11 km/sec (see also Table 9).

Factors Affecting Penetration Characteristics

The way in which velocity changes with altitude during the fall depends upon several factors:

I. Approach characteristics (Figure 13):
velocity of approach, v_∞
angle of approach, ϕ

The velocity and angle of atmospheric approach are primary factors in determining the severity of the entry deceleration and heating. The dangerous combination of high velocity at low altitude is most apt to occur when the initial velocity is high or when the entry is perpendicular, that is $\phi = 90°$.

II. Meteorite characteristics. The important value is the drag/mass ratio, DA/m, or $3D/4rd$. For the same shape, the smaller density and thus larger drag/mass ratio of a stone meteorite allows deceleration to occur in the higher, less dense region of the atmosphere, making the heating rate less severe than for an iron meteorite. A slender body has a low drag/mass ratio and would penetrate further into the atmosphere than blunt bodies with higher drag/mass ratios. If the body is shield formed, appreciable lift forces may develop which can force the meteorite into a more shallow path and thereby cause deceleration to occur at high altitudes.

III. Atmospheric characteristics. For hydrostatic equilibrium in an isothermal atmosphere it follows from Boyle's law that the atmospheric density ρ at the altitude z km is

$$\rho = \rho_0 \exp(-az) = 0.0084 \cdot \exp(-0.143z)$$

where ρ_0 is the density at sea level in g/cm^3, exp is the base of natural logarithms and a is a constant dependent upon the temperature and composition of the atmosphere. From rocket and satellite experiments we now have a good knowledge of a, and although the atmosphere is far from isothermal, an expression of the above type represents Earth's atmosphere well up to about 150 km (Jacchia 1971).

Calculations

Let us consider the case of a meteorite that makes a vertical entry from space at a velocity v and an angle

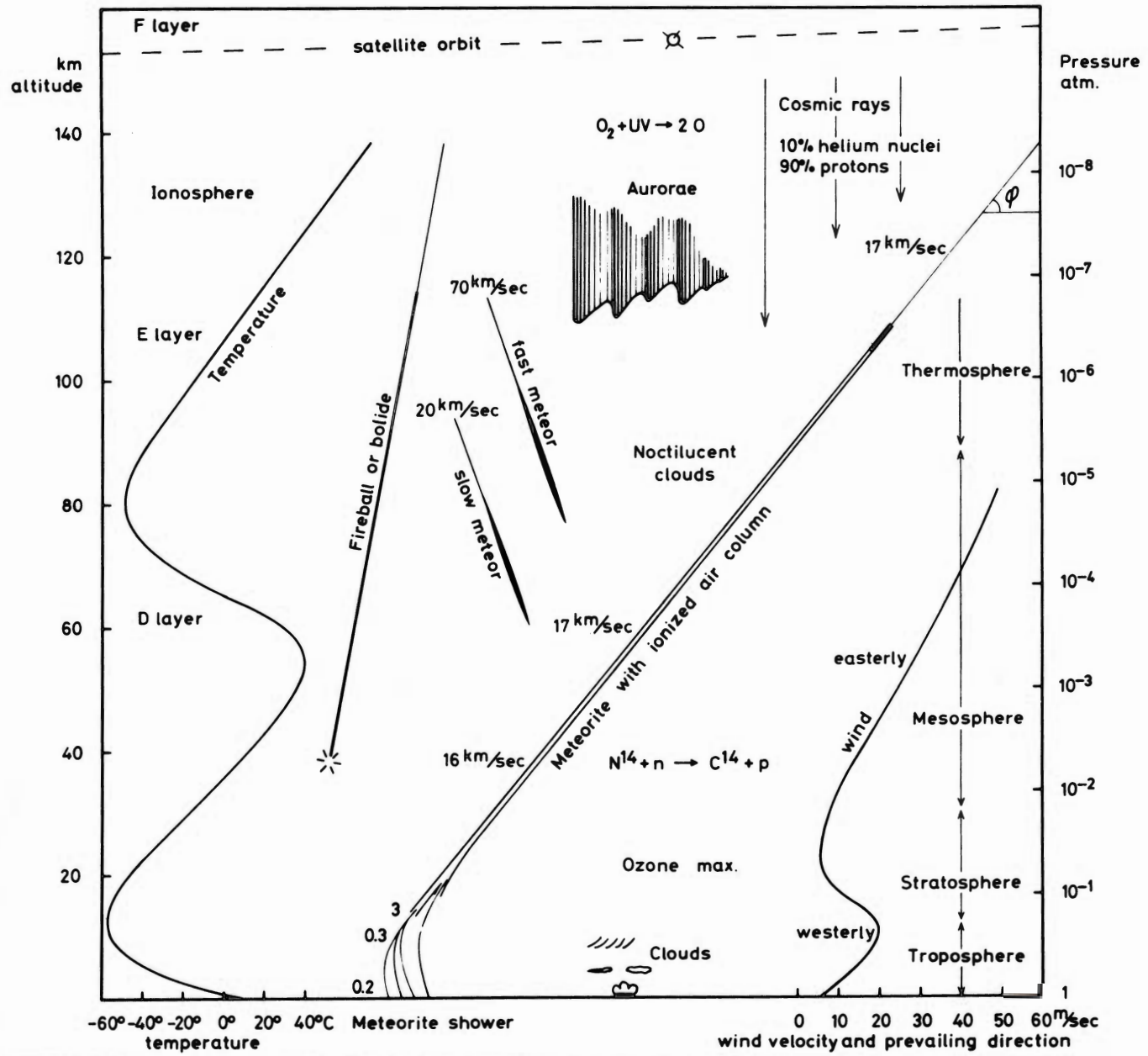

Figure 13. Schematic presentation of the Earth's atmosphere and some common events. The decreasing pressure (right hand axis) is shown versus altitude in km (left hand axis). Typical temperature profiles and wind velocities for 45° northern latitude are shown. It will be noted that the meteorite's trajectory may be strongly influenced at low altitudes by winds.

$\phi = 90°$. To a first approximation we will assume that the drag coefficient and the mass are constant. We can then apply equation (1).

$$\frac{dv}{dt} = -\frac{DA}{m}\,\rho v^2$$

In this we substitute $\rho = \rho_0 \exp(-az)$

$$\frac{dv}{dt} = -\frac{DA\rho_0}{m}\,v^2 \exp(-az) = -Bv^2 \exp(-az) \qquad (2)$$

But the velocity in relation to the Earth is $v = -\frac{dz}{dt}$, and $\frac{dv}{dt}$ may be written

$$\frac{dv}{dt} = \frac{dv}{dz} \cdot \frac{dz}{dt} = -v\,\frac{dv}{dz}$$

This result is substituted in (2):

$$-v\,\frac{dv}{dz} = -Bv^2 \exp(-az)$$

$$\frac{dv^2}{dz} - 2Bv^2 \exp(-az) = 0$$

This is an inhomogeneous linear differential equation of first order in v^2, which has the following standard solution:

$$v^2 = k \exp\left[-\int -2B \exp(-az)dz\right] = k \exp\left[-\frac{2B}{a}\exp(-az)\right] .$$

To find the constant k we note that for $z \to \infty, \exp(-az) \to 0$, therefore

$$\exp\left[-\frac{2B}{a}\exp(-az)\right] \to 1$$

and $v \to v_\infty$; thus $k = v_\infty^2$. The full solution may then be written

$$v^2 = v_\infty^2 \exp\left[-\frac{2B}{a}\exp(-az)\right]$$

or

$$v = v_\infty \exp\left[-\frac{B}{a}\exp(-az)\right]$$

or

$$v = v_\infty \exp\left[-\frac{DA\rho_0}{ma}\exp(-az)\right] .$$

If the approach angle ϕ deviates from 90°, a correction factor must be applied and the equation becomes

$$v = v_\infty \exp\left[-\frac{DA\rho_0}{ma\sin\phi}\exp(-az)\right]$$

or

$$\frac{v}{v_\infty} = \exp\left[-\frac{DA}{m\sin\phi}\frac{\rho_0}{a}\exp(-az)\right] \qquad (3)$$

Figure 14 illustrates the velocity variation with altitude, z km, for several values of the parameter K:

$$K = \frac{DA}{m\sin\phi} = \frac{0.75\,D}{r\,d\sin\phi} \qquad (4)$$

where r is the initial radius of the body, and d its density.

The curves are interesting by their sigmoid form. They are all of the same shape, which means that a stone meteorite, an iron meteorite, a shooting star and a satellite all lose the same fraction of the original velocity within a certain vertical distance. The decrease from 95% to 5% of the cosmic velocity thus takes place within a stratum of the atmosphere of 28 km thickness; however, these 28 km may be situated in the ionosphere for a light body (K large) but close to the Earth's surface for a heavy body (K small). For very small K values, i.e., large masses at perpendicular entry, the approaching body will impact the surface of the Earth with near its cosmic velocity. For example an iron meteorite of 3,600 tons, with a radius of 480 cm, at vertical entry will theoretically follow the curve for $K = 0.0001$ and thus hit the surface of the Earth with 92% of its cosmic velocity. This will undoubtedly lead to severe cratering of the Earth.

It would have been interesting to test the equations on iron meteorites. However, iron meteorite falls are extremely rare (Table 10), and insufficient observational data are

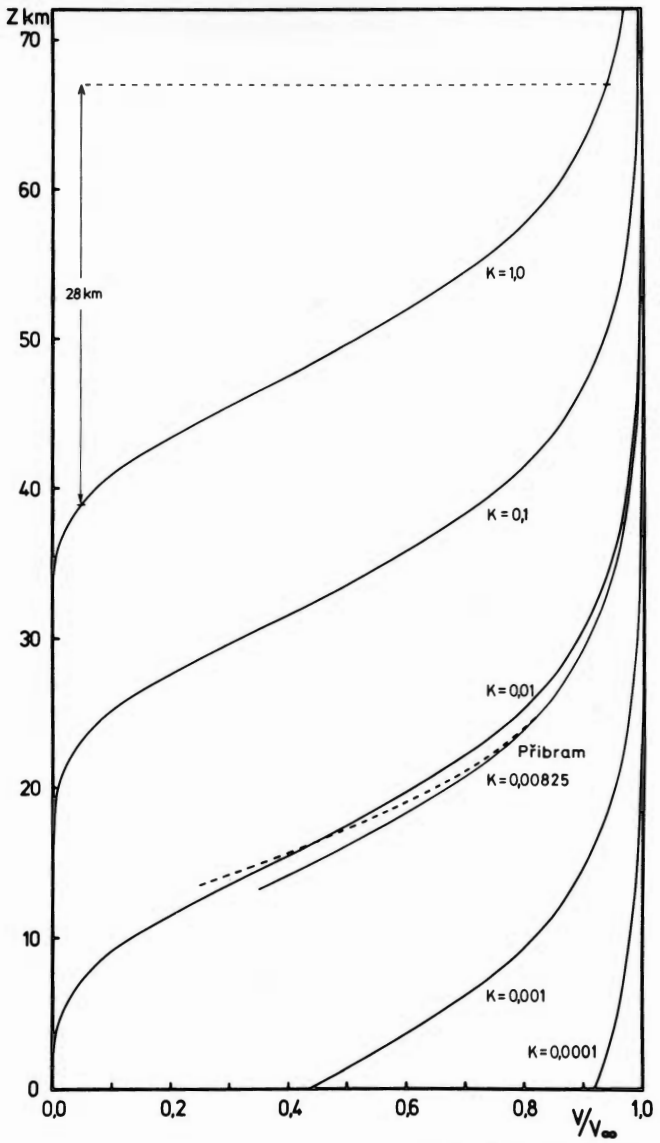

Figure 14. The velocity of a meteorite in the Earth's atmosphere as a function of altitude. Instead of actual velocities, the ratio between velocity at any given time, v, and the initial velocity, v_∞, is shown. The parameter K is discussed in the text.

available. For the stone meteorite Přibram, Ceplecha (1961) has reported all relevant data and calculated its fall by an elaborate method. For comparison, I have applied the approximate method developed here to illustrate Přibram's fall, using Ceplecha's observational data. The initial velocity, v_∞, was 20.89 km/sec and the approach angle, ϕ, was 43°. The initial mass is unknown but here assumed to have been 100 kg (about 10 kg has been found). The density is 3.5 g/cm^3, and the drag coefficient is estimated to be 0.5. Thus, from equation (4)

$$K = \frac{0.75 \times 0.5}{19.0 \times 3.5 \times 0.682} = 0.00825$$

The resulting curve v/v_∞ versus altitude, Figure 14, almost coincides with the curve estimated by Ceplecha, demonstrating the validity of the simplifying assumptions.

To estimate the effect of ablation on the trajectory, let us assume that the Přibram body diminished from 100 kg to 50 kg during the flight from an altitude of 96 km down to an altitude of 13.3 km where the trail ceased to be luminant. In this case, the radius decreased from 19.0 to 15.1 cm, and consequently K increased from 0.00825 to 0.0104. As a result of ablation, the trajectory would thus gradually have shifted from the first calculated curve to one similar to the curve $K = 0.01$, as indicated in Figure 14. Of course, matters are further complicated by the frailness of the incoming body. Instead of considering one body that smoothly decelerates and ablates, we often have to work with multiple falls; i.e., cases where the meteorite fragmentates once, or more, during the atmospheric flight. Přibram was, in fact, such a case; Ceplecha estimated from the photographs that at least 17 fragments were produced; at the time of his writing only four of these had been found, but an additional 15 specimens have later been recovered (Hey 1966).

For Přibram's trajectory we found the K-value to be 0.00825. It is interesting to note that the same flight characteristics, v/v_∞ versus altitude, may be obtained for other meteorites, given the proper combination of r, d and ϕ. To illustrate this we solve equation (4)

$$\frac{0.75\,D}{r\,d\,\sin\phi} = 0.00825$$

for different r, d and ϕ; see Table 8.

From the data of the table, we gather that an iron meteorite of, e.g., 885 kg may show the same v/v_∞ values as the 100 kg Přibram stone. It is, however, required that the iron enters the atmosphere at a much lower angle, and it will consequently have a much longer trajectory. In the case mentioned, the trajectory will be about 3.5 times longer and the flight time will also be 3.5 times longer; i.e., the deceleration will be softer. Such an iron will probably display a larger proportion of effectively smoothed surfaces, with fewer regmaglypts, than one which plunges steeply into the atmosphere, see page 47.

Table 8. Přibram and Three Hypothetical Iron Meteorites with the Same K-value, 0.00825, and therefore with the Same v/v_∞ Characteristics as Přibram in Figure 14

	Initial mass, kg	Initial radius, cm	Density g/cm^3	Angle of approach
Stone meteorite, Přibram	100	19.0	3.5	43°
Iron meteorite A	6.5	5.83	7.8	90°
Iron meteorite B	20.4	8.55	7.8	43°
Iron meteorite C	885	30.0	7.8	11°.2

In recent years several experiments with artificial meteorites have been successfully accomplished. In 1966 a 5.7 gram, 0.2% C-steel pellet was thus carried into the ionosphere by a six-stage, solid fuel Trailblazer II rocket and launched back towards the Earth from an altitude of 120 km (Robertson & Ayers 1968). The meteor – and its burned out rocket stages – were photographed with a system of cameras and spectrographs. The initial velocity of the steel pellet was 10.85 km/sec; it penetrated to a height of 70 km before it became visible as a meteor. After a brief flare of 0.9 sec. duration, it again disappeared at a height of 61 km, apparently having completely disintegrated. Experiments of this kind are valuable because they provide a meteor light source of known composition, density, and shape, with the aid of which photographs and spectrograms of natural meteors may be calibrated. Some of the most recent results have been reported by Ayers et al. (1970).